Fundus eye images, frequency domain,
spectral fractal dimension

Maria BERNDT-SCHREIBER*, Anna BĄCZKOWSKA*

NUMERICAL ANALYSIS OF FUNDUS EYE IMAGES IN FREQUENCY DOMAIN

A new approach in the analysis of fundus images performed in frequency domain is described. It is related to specific features of the power spectrum and refers to the notion of spectral fractal dimension as well. Preliminary calculations have been carried out for sample series of diagnosed fundus eye images. The results and proposals for further improvements of the method are discussed.

1. INTRODUCTION

Due to the possible relation to various pathological changes, the need of bias-free description of fundus eye images remains a crucial challenge in diagnosing procedures [15,19,20]. Quantitative description of the fundus eye images becomes essential not only for ophthalmologists – the observations and assessments of these images for detection and monitoring pathological changes are also of importance for nephrology and neurology experts nowadays [13,22].

Despite recent technological advances proper diagnosing procedures for fundus images are extremely sophisticated and methodological investigations are carried on regularly in many clinical centers (comp. e.g. [2,11,12]). In Figure 1, below, two sample fundus images from our database are presented for normal and pathological cases, respectively.

Our ultimate goal is to elaborate appropriate methodological approach to the quantitative analysis of the fundus images. It is commonly accepted that the Fourier analysis in digital imaging may help to reveal many essential features not easily observable in the space domain [7,10]. The complex texture of retinal patterns and, in general, many other complicated biological structures have often been treated both in the space and frequency domains as fractal-like objects [1,3,8-9,14-18,21]. Below we present a proposal of a numerical analysis of fundus images in the frequency domain, focusing on the power spectrum shapes and referring to the fractal dimension estimation as a measure of the structure complexity on the one hand, and a possible classifying parameter supporting the diagnosing methods on the other hand. The study is complementary to our previous attempts [3-6]. Preliminary calculations are performed on sample collected image data relevant to various pathologies and some future extensions of the approach are outlined.

* Faculty of Mathematics and Computer Science, Nicolaus Copernicus University, Toruń, Poland

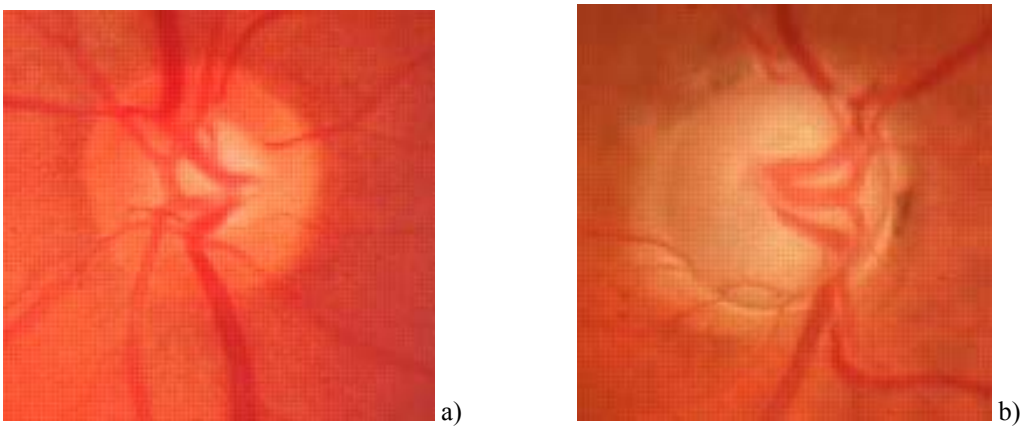

a) b)

Fig. 1. Sample fundus image: a normal case(a) and a pathological case (glaucaoma) (b).

2. METHODS AND MATERIALS

2.1. METHODS OF CALCULATIONS

When interpreting the image data in the frequency domain we are interested in the amplitude at each frequency – which is given by power spectrum. It is observed that the Fast Fourier Transform (FFT) images of the optic disc areas may reveal specific individual features and therefore their quantitative description may be essential for diagnoses. Sample images of different shapes are shown in Figures 2 and 3, below. In our approach we perform numerical analysis of the power spectrum of fundus images and the central idea is to view an image in the frequency domain as a collection of iso-intensity contours.

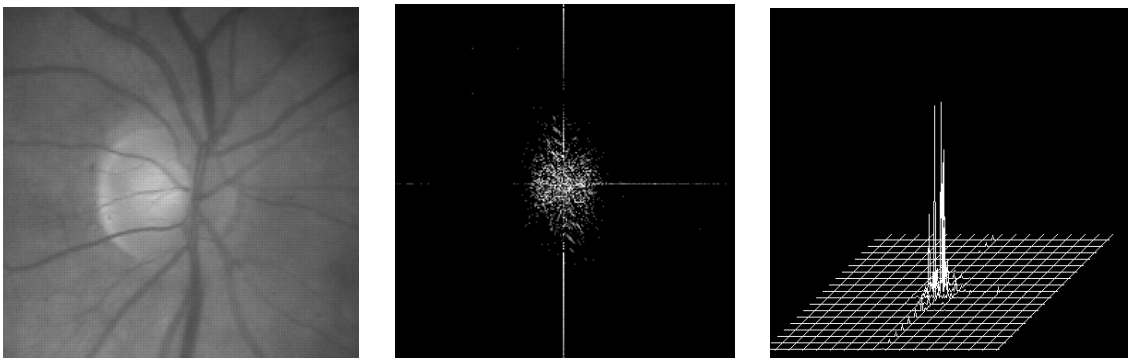

a) b) c)

Fig. 2. Sample images: original fundus image (a) and its cross-like power spectrum in 2D (b) and 3D (c) representations.

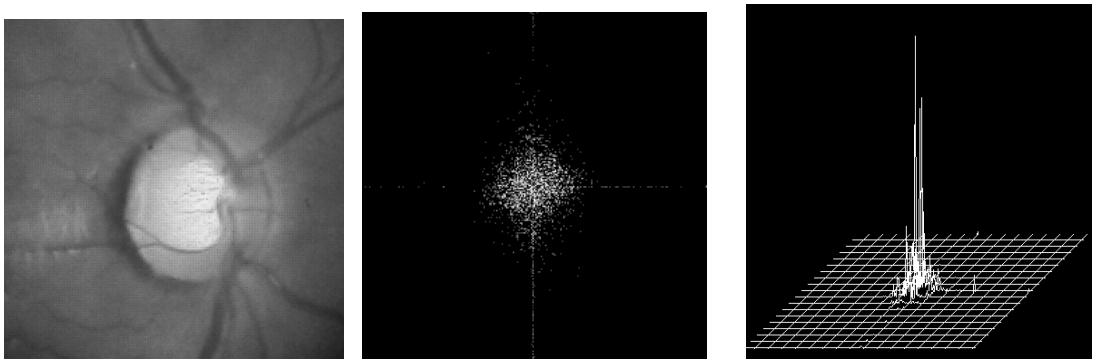

d) e) f)

Fig. 3. Sample images: original fundus image (d) and its circular power spectrum in 2D (e) and 3D (f) representations.

We assume the power spectrum F is described as

$$F(x,y) = C\, r^{\{-beta\}}, \qquad (1)$$

where $r^2 = x^2+y^2$.

We treat the relation in a flexible way, assuming in practice that the graph of the power spectrum may be represented as well by a cone surface with a basis being not of a regular circular shape, and with the center being possibly shifted from the zero position. Notice, that at a given height ***h*** the level set of points *(x,y)* for which $F(x,y)\geq h$ will be a disc of radius ***r*** satisfying the relations below:

$$C\, r^{-beta} = h \quad \rightarrow \quad r = C^{1/beta}\, h^{-1/beta} \quad . \qquad (2)$$

Eventually, the number of pixels in the level set of height *h* will be of the order of the surface *S* of the circle, i.e. $\pi C^{2/beta}\, h^{-2/beta}$. For a more general case **(**for different shapes of the cone's bases, and different values of the constant *C***)** it may be stated that the number of pixels at the *h* level set is given by the following formula:

$$S(h) = C'\, h^{-2/beta} \quad , \qquad (3)$$

where C' is unknown.

Taking logarithms of both sides of the equations we get a linear relation**:**

$$log\ S(h) = log\ C' - [2/beta]\ log\ h \qquad (4)$$

We skip the coefficient *log C'* and calculate the coefficient $a = -2/beta$ using the least squares method to find *beta.*

It may happen (as shown above for various power spectra) that the shape of the basis will not be a regular circle but rather of a cross shape. Then the relation for *S(h)* should be of the form:

$$S(h) = C' h^{-1/beta}. \quad (5)$$

Here the number of pixels is roughly estimated using the scaling factor of the form $h^{-1/beta}$ describing an object of type 1D. Thus we have the final formula as follows:

$$log\ S(h) = log\ C' - [1/beta]\ log\ h. \quad (6)$$

And we calculate the coefficient $a = -1/beta$ using the least squares method to find *beta*, similarly as above.

Finally the algorithm consists of the following steps:

1. calculate the power spectrum F(x,y)
2. calculate M:=max_(x,y) F(x,y)
3. choose alternatively either A. or B.
   A. linear scale:
      for k = 1 to N (Number_of_node points)
      $u[k]$ = log(0.1**M* + *k**0.8**M/N*);
      $v[k]$ = surface of the level set at height exp*(u[k])*
   B. logarithmic scale:
      for k = 1 to N (Number_of_node_points)
      *u[k] = log M - 0.3 - 2*k/N;*
      $v[k]$ = surface of the set level at height exp*(u[k])*
4. find with the least square method the coefficient a in the relation $v=a*u+b$ for u and v as above
5. if the basis of the cone surface is of the circular shape
   return *beta:=-2/a;*
   if the basis of the cone surface is cross-shaped
   return *beta:=-1/a;*

Note that the term *linear scale* above refers to spacing between the values *v[k]* determining the heights at which the level sets are probed, rather than to *u[k]'s* coinciding with *log v[l]*. Likewise, the *logarithmic scale* means the spacing between *u[k]'s* varies exponentially. Observe also that we cut off the extreme values (close to *0* or *M*) on both scales in order to avoid possible numerical instabilities in their vicinity. We made a particular choice of the constants in the formulae for *u[k]* and *v[k]* above, but in general they can be regarded as parameters of the algorithm. Finally our approach refers to the notion of spectral fractal dimension *Ds* as related to a quantitative description of power spectrum and estimated as follows [17]:

$$Ds=(7-beta)/2. \quad (7)$$

2.2. IMAGE DATA

In the present studies we investigate original images of optic discs areas of fundus images collected in the Ophthalmology Ward of the Rydygier Hospital in Toruń. All the images are taken in routine non-invasive examinations with only the pupils dilated in order

to reveal the entire optic disc areas and the surfaces of retinal vessel patterns. Philips ESP2/200 digital camera combined with a Zeiss Retinophot Fundus Camera is used for the purpose. The collected image data together with additional medical information data are directly transferred from the Ophthalmology Ward to the University server. The calculations reported below have been carried out for two separate sets of images. The first one – applied for test calculations checking only the stability of the algorithm - consisted of 54 fundus images: referring to 37 hospital patients and 17 members of the control group, with 26 men and 27 women at the age of 21 to 86 years. The second set consisted of 20 images selected as the ones with full diagnosing descriptions, covering 11 men and 9 women at the age of 20 to 85. The confirmed diagnoses for the studied group were equally represented by five cases of each of the following pathologies: glaucoma, diabetics and hypertension. Five cases have been recognized as normal.

3. RESULTS AND DISCUSSION

3.1. TESTS OF THE ALGORITHM

Test calculations have been performed to check the stability of the algorithm – in particular the choices of the number of nodes and the defined scales (either logarithmic or linear) referring to the spacing chosen in the calculations scheme outlined above have been tested. Sample typical results are represented on graphs in Figures 4 and 5, below, which indicate the analysis of images of the size 256 x 256 with the choice of 1000 nodes sounds reasonable for any choice of spacing.

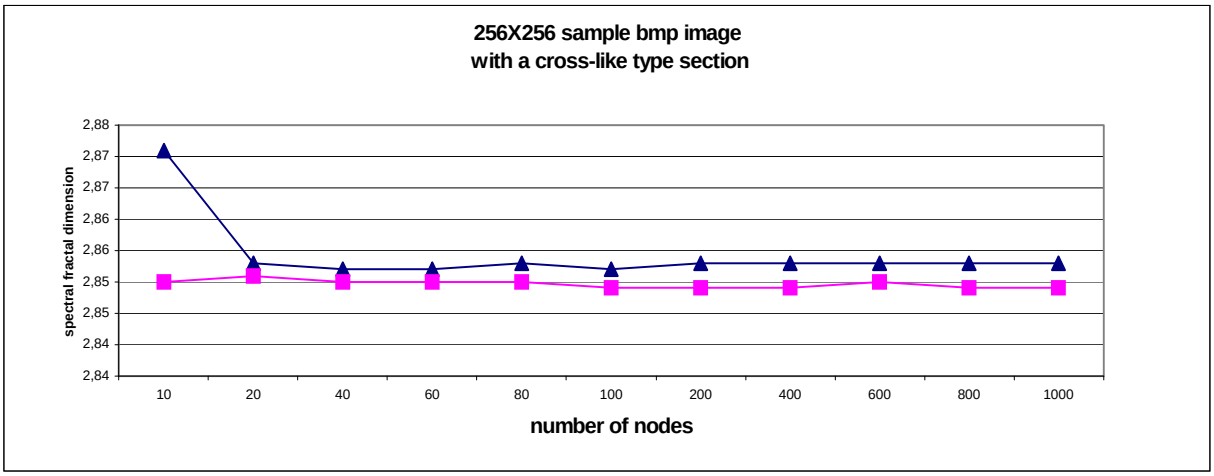

Fig. 4. Sample graphs presenting the results of testing calculations of spectral fractal dimension values Ds for selected *bmp* images of cross-like shapes of power spectrum sections. Numbers of nodes have been equal to 1000, and two types of spacing have been chosen: linear shown as triangles and logarithmic shown as squares (see the text for details).

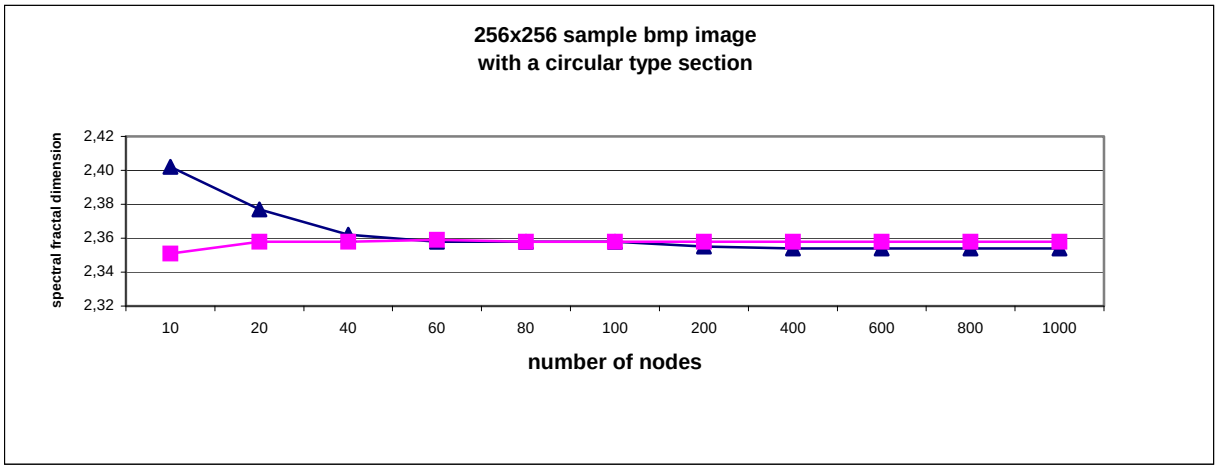

Fig. 5. Sample graphs presenting the results of testing calculations of spectral fractal dimension values Ds for selected *bmp* images of cicular shapes of power spectrum sections. Numbers of nodes have been equal to 1000, and two types of spacing have been chosen: linear shown as triangles and logarithmic shown as squares (see the text for details).

3.2. RESULTS FOR DIAGNOSED FUNDUS IMAGES

With the assumptions resulting from the above testing procedures the calculations have been carried out for the selected set of 20 images with the confirmed diagnosing descriptions (comp. section 2.2). The results of the calculations are presented in Table 1, below, where the values of spectral fractal dimensions Ds and the absolute value of the coefficient *a* (comp. the algorithm outline step 4) are listed together with images codes and diagnoses. Additionally, the values of the parameter C/D are shown for the images under study. The C/D parameter refers to the cup (C) to disc (D) areas ratio estimations based on direct measurements performed for digital fundus images [5-6,11-12]. It is commonly accepted that the value of C/D indicates the state of nerve disc; in most cases the value below 0.3 is observed for normal cases.

Table 1.Calculations results for spectral fractal dimensions *Ds* and coefficient *a* for diagnosed images compared with the C/D parameters values based on measurements (see details in the text).

Image code	Diagnosis	Parameter C/D (based on measurements)	Absolute value of parameter |a|	Spectral fractal dimension D_s
1	diabetics	0,17	0,69	2,78
2	diabetics	0,10	0,78	2,86
3	diabetics	0,10	0,72	2,81
4	diabetics	0,09	0,77	2,85
5	diabetics	0,10	0,75	2,83
6	glaucoma	0,45	0,89	2,94
7	glaucoma	0,53	0,64	1,94
8	glaucoma	0,48	0,67	2,01
9	glaucoma	0,37	0,77	2,85
10	glaucoma	0,54	0,75	2,16
11	hypertension	0,28	0,80	2,88
12	hypertension	0,11	0,80	2,88
13	hypertension	0,09	0,79	2,24
14	hypertension	0,14	0,73	2,82
15	hypertension	0,11	0,66	2,74
16	normal	0,27	0,87	2,94
17	normal	0,17	0,74	2,82
18	normal	0,31	0,87	2,92
19	normal	0,13	0,73	2,82
20	normal	0,19	0,79	2,87

It is interesting to note that the correlation coefficients between the values of C/D and Ds, considered separately for the four different diagnosed groups, appear quite reasonable as shown in Table 2, below.

Table 2. Correlation coefficients between the values of spectral fractal dimensions Ds and the C/D parameters – estimated separately for the four groups of pathologies in the images listed in Table 1.

Cases	Correlation coefficient Ds versus C/D
diabetics	-0.85
glaucoma	-0.79
hypertension	0.52
normal	0.92

4. CONCLUSIONS

The presented preliminary results confirm the proposed method might be useful in the procedure of classifying the images in the diagnosing procedures. However, it does require further investigations. In particular, we are planning to apply the algorithm to colour images in three channels and also to check its applicability to the Fourier transforms performed in

polar coordinates which seem more appropriate for the study of nerve disc areas in the fundus images.

BIBLIOGRAPHY

[1] AHAMMER H., DEVANEY T., T., J., TRITTHART H. A, Fractal Dimension of K1735 Mouse Melanoma Clones and Spheroid Invasion in Vitro, Eur. Biophys. J. Vol. 30, 494-499, 2001.

[2] BANES M. J., CULHAM L. E., CROWSTON J. G., BUNCE C., KHAW P.T., An Optometrist's Role in a Hospital Glaucoma Clinic, Ophthal. Physiol. Opt. 20, 351-359, 2000.

[3] BERNDT-SCHREIBER M., BIEGANOWSKI L., Fractal Analysis of Serial Fundus Images for Retinal Disease Monitoring, Machine Graphics & Vision Vol. 9, 433-438, 2000.

[4] BERNDT-SCHREIBER M., MIKOŁAJCZAK I., Fourier Based Analysis of Fundus Eye Images, [in] Computer Recognition Systems KOSYR 2001, (Eds) M. Kurzyński , E. Puchała, M. Woźniak, Division of Systems and Computer Networks, Wrocław University of Technology, Wrocław 2001, pp. 43-47

[5] BERNDT-SCHREIBER M., BIEGANOWSKI L, KOWALCZYK A., MACIEJEWSKI K.**,** Digital Analysis of Ophthalmological Images – a Proposal for a Screening Strategy, Polish J. Med. Phys.& Eng., Vol.8 (2), pp. 89-98, 2002.

[6] BERNDT-SCHREIBER M., BIEGANOWSKI L., BROŻEK M., KOWALCZYK A., MACIEJEWSKI K., Biomorphological Measurements Based on Digital Fundus Eye Images, Int. J. Applied Mathematics and Computer Science (accepted for publication 2003)

[7] BRACEWELL R.N., Fourier Analysis and Imaging, Kluwer / Academic Publishers 2003

[8] DAXTER A., Characterisation of the Neovascularisation in Diabetic Retinopathy by Means of Fractal Geometry: Diagnostic Implications ,Grafe's. Arch. Clin. Ophthalmol., Vol. 231(12), pp. 681-686, 1993.

[9] DAXTER A., The Fractal Geometry of Proliferative Diabetic Retinopathy: Implications for the Diagnosis and the Process of Retinal Vasculogenesis, Curr. Eye Res. Vol. 12(12), pp. 1103-1109, 1993

[10] GONZALEZ R., WOODS R., Digital Image Processing , Prentice Hall 2002

[11] GILCHRIST J., Optometric Glaucoma Referrals – Measures of Effectiveness and Implications for Screening Strategy Ophthal. Physiol. Opt. Vol. 20, 452-463, 2000

[12] HARPER R., REEVES B., SMITH G., Observer Variability in Optic Disc Assessment: Implications for Glaucoma Shared Care, Ophthal. Physiol. Opt. Vol. 20, 265-273, 2000

[13] HUBBARD L.D., BROTHERS R.J., KING W.N., CLEGG L.X., KLEIN R., COOPER L.S., SHARRETT A.R., DAVIS M.D., CLAI J., Method for Evaluation of Retinal Microvascular Abnormalities Associated with Hypertension/Sclerosis, Ophthalmology Vol. 6(12), 59-80,1999

[14] KYRIACOS S., NEKKA F., VICCO P., CARTILIER L., The Retinal Vasculature: Towards an Understanding of the Formation Process [in] Fractals in Engineering, (Eds.) Levy Vehel J., E. Lutton E., Tricot C., Springer pp. 383-397, 1997.

[15] LAMMINEN H., RUOHONEN K. Fundus Imaging and the Telemedical Management of Diabets, J. Telemed Telecare Vol. 8(5), 255-258, 2002

[16] LANDINI G., MISSIONS G. P., MURRAY P.I., Fractal Analysis of the Normal Human Retinal Fluorescein Angiogram, Curr. Eye Res. Vol. 12(1),.23-27, 1993

[17] LOSA G.A., MERLINI D., NONNENMACHER T.F.,WEIBEL E.R.(eds), Fractals in Biology and Medicine, Birkhause, Basel, Boston, Berlin 1998

[18] MORFILL G., BUNK W., New Designs on Complex Patterns, Europhysics News, Vol. 32, pp. 123-136, 2001.

[19] PORTA M., BANDELLO F., Diabetic Retinopathy. A Clinical Update, Diabetologia, Vol.45, .1617-1634, 2002

[20] SINATHANAYAOTHIN C., BOYCE J. F., WILLIAMSON T .H., COOK H. L., MENSAH E., LAL S., USHER D., Automated Detection of Diabetic Retinopathy on Digital Fundus Images, Diabetic Medicine Vol. 19, 105-112, 2002

[21] TOURASSI G., FREDERICK E. D., VITTITOE N. F., COLEMAN R. E., Fractal Texture Analysis of. Perfusion Lung Scans, Computers and Biomedical Res. Vol. 33, pp.161-171, 2000.

[22] WONG T.Y., KLEIN R., KLEIN B. E., TIELSCH J.M., HUBBARD L., NIETO F.J., Retinal Microvascular Abnormalities and their Relationship with Hypertension, Cardiovascular Disease and Mortality, Survey of Ophthalmology Vol. 46(1), 59-80, 2001